Ecosystems
https://doi.org/10.1007/s10021-025-01008-0

ORIGINAL ARTICLE

Woody Encroachment Intensifies Deep Soil Drying at Daily, Seasonal, and Decadal Scales

Karla M. Jarecke,[1,2]* Rachel M. Keen,[3] Kamini Singha,[4] Jesse B. Nippert,[5] Sharon A. Billings,[3] Xi Zhang,[6] Kayalvizhi Sadayappan,[7] Matthew F. Kirk,[8] Daniel R. Hirmas,[9] Li Li,[7] Hoori Ajami,[10] Marc Dumont,[4] Alejandro N. Flores,[11] and Pamela L. Sullivan[2]

[1]*Department of Geography, Institute of Arctic and Alpine Research, University of Colorado Boulder, Boulder, Colorado, USA;* [2]*College of Earth, Ocean, and Atmospheric Sciences, Oregon State University, Corvallis, Oregon, USA;* [3]*Department of Ecology & Evolutionary Biology and Kansas Biological Survey & Center for Ecological Research, University of Kansas, Lawrence, Kansas, USA;* [4]*Hydrologic Science and Engineering Program, Colorado School of Mines, Golden, Colorado, USA;* [5]*Division of Biology, Kansas State University, Manhattan, Kansas, USA;* [6]*Department of Biosystems Engineering and Soil Science, University of Tennessee-Knoxville, Knoxville, Tennessee, USA;* [7]*Department of Civil and Environmental Engineering, The Pennsylvania State University, University Park, Pennsylvania, USA;* [8]*Department of Geology, Kansas State University, Manhattan, Kansas, USA;* [9]*Department of Plant and Soil Science, Texas Tech University, Lubbock, Texas, USA;* [10]*Department of Environmental Sciences, University of California Riverside, Riverside, California, USA;* [11]*Department of Geosciences, Boise State University, Boise, Idaho, USA*

Abstract

The conversion of grasslands to shrublands, known as woody encroachment, has increased vegetation water use, particularly in mesic systems. However, declines in soil moisture due to woody encroachment have not been extensively explored. This study examines the impacts of woody encroachment on the depth and degree of soil drying in a mesic tallgrass prairie in Kansas, USA. We compared soil drying beneath roughleaf dogwood (*Cornus drummondii*) and non-encroached tallgrass prairie using half-hourly measurements of soil moisture from 2021 to 2024 (event scale), electrical resistivity in June and October of 2022 (seasonal scale), and neutron probe measurements collected monthly between 1984 and 2021(decadal scale). Across all time scales, we found increased soil drying beneath shrubs compared to grasses, particularly in deeper layers. Soil moisture declined up to 20% more at 60 cm depth beneath shrubs compared to grasses after individual storm events, whereas declines at 15 cm were similar beneath shrubs and grasses. Electrical resistivity imaging suggested double the depth and degree of seasonal soil drying beneath shrubs compared to grasses. Over nearly four decades, woody-encroached catchments experienced a greater degree of soil drying than grass-dominated catchments, especially at depths below 1 m. The intensification of soil drying, combined with larger storms in mesic grasslands, is likely to have consequences for deep

Received 26 March 2025; accepted 29 August 2025

Supplementary Information: The online version contains supplementary material available at https://doi.org/10.1007/s10021-025-01008-0.

Author Contributions Karla M. Jarecke, Rachel M. Keen, Kamini Singha, Jesse B. Nippert, Pamela L. Sullivan, Sharon A. Billings, Daniel R. Hirmas, Li Li, Hoori Ajami, and Alejandro N. Flores contributed to conceptualization and design of the study. Karla M. Jarecke and Rachel M. Keen contributed to data analysis and writing. Karla M. Jarecke, Pamela L. Sullivan, Jesse B. Nippert, and Xi Zhang collected the data. All authors contributed to the review and editing of the manuscript.

*Corresponding author; e-mail: karla.jarecke@colorado.edu

Published online: 29 September 2025

carbon storage and export and for groundwater recharge in woody-encroached grasslands.

Key words: woody-encroached grasslands; soil moisture; soil drying; electrical resistivity tomography; roots; plant water use strategies; moisture whiplash.

Highlights

- Soil moisture decline after storms was up to 20% greater under shrubs than grasses.
- Resistivity images showed twice the depth of soil drying under shrubs than grasses.
- Woody encroachment increased deep (> 1 m) soil drying over nearly four decades.

Introduction

Grasslands and savannas worldwide are experiencing woody plant encroachment, defined by the increase in native woody plant cover in grass-dominated ecosystems (Honda and Durigan 2016; Stevens and others 2017; Schmidt and others 2024). As woody shrubs expand into grasslands, the effects on infiltration, plant water use, and streamflow can vary depending on environmental conditions including climate, bedrock composition, and soil characteristics (Huxman and others 2005; Acharya and others 2018; Zou and others 2018; Deng and others 2021; Wilcox and others 2022). These complexities have prompted several studies aimed at improving our process-based understanding of subsurface hydrology in woody-encroached landscapes (Acharya and others 2017b; Vero and others 2017; Sullivan and others 2019; Wen and others 2022; Jarecke and others 2024). Moreover, accounting for the ecohydrological linkages associated with vegetation change is critical for disentangling the effects of woody encroachment and climate change on water yields (Schreiner-McGraw and others 2020; Sadayappan and others 2023). For example, in mesic tallgrass prairie of the central USA, woody-encroached catchments experienced significant stream drying despite an increase in precipitation over the last few decades (Keen and others 2023). While the decline in streamflow is associated with increased evapotranspiration by woody plants compared to grasses in mesic climates (Zou and others 2014; Logan and Brunsell 2015; Dodds and others 2023; Keen and others 2023, 2024b; Sadayappan and others 2023), the degree, and thus importance, of deep subsurface drying in response to climate and woody plant encroachment is not well understood (Ilstedt and others 2016; Acharya and others 2017a; Niemeyer and others 2017).

Physiological and morphological differences between grasses and woody plants, including shrubs and trees, influence their water use strategies, affecting both the depth and amount of soil water depletion. Woody plants are known to maintain higher transpiration rates than grasses both in upland landscapes (O'Keefe and others 2020; Keen and others 2023) as well as riparian corridors (Scott and others 2006). They typically have a higher leaf area index than grasses (Tooley and others 2022), providing more surface area for carbon and water exchange. Woody shrubs also develop root systems capable of efficiently using near-surface soil water (O'Keefe and others 2022) while also producing extensive coarse-root systems that can extend over 2 m into the soil profile (Ratajczak and others 2011). C_4 grasses of tallgrass prairie can also be deeply rooted, but they concentrate the majority of their roots in surface soils and, as a result, rely almost exclusively on shallow soil moisture (0 to 30 cm; Nippert and others 2012). In contrast, shrubs exhibit plasticity in their depth of water uptake within individual growing seasons, primarily accessing deeper water sources during dry conditions to reduce competition with grasses (Keen and others 2024a, 2024b; Nippert and Knapp 2007; Ratajczak and others 2011). Additionally, the coarse woody roots of shrubs and trees create channels that facilitate the preferential flow of water to deeper soil layers (Guo and others 2020; Jarecke and others 2024), which may benefit them long term by promoting root growth and access to nutrients over a greater soil volume (Johnson and Lehmann 2006).

The contrasting water use strategies of grasses and woody plants in woody-encroached grasslands directly influence soil-moisture variability. Changes in both long-term soil-moisture availability and short-term fluctuations can significantly impact subsurface hydrological processes, including groundwater recharge (Schreiner-McGraw and others 2020). These changes also regulate microbial processing of soil organic matter (Maggi and Porporato 2007; Tiemann and Billings 2011) and the export of carbon and nutrients (Macpherson and Sullivan 2019; Sullivan and others 2019; Wen and others 2020, 2022) at hourly to seasonal timescales. Over longer time periods, woody encroachment in mesic grasslands has been associated with increased

loss of soil organic carbon (Jackson and others 2002) as well as the accumulation of soil organic carbon (Li and others 2019). However, the mechanisms remain unclear. Thus, understanding changes to soil drying with land cover change over multiple temporal scales is important to connect short-term carbon and nutrient production and mobilization to long-term ecosystem carbon budgets.

Here, we investigate the influence of woody encroachment on soil drying in a native tallgrass prairie of the North American Central Great Plains. Specifically, we quantified the depth and degree of soil drying beneath shrubs and grasses over event, seasonal, and decadal scales. We analyzed three years of half-hourly soil-moisture measurements, repeated electrical resistivity surveys conducted during one growing season, and 37 years of monthly neutron probe soil-moisture measurements. These data were collected from catchments experiencing significant shrub encroachment, as well as from catchments where annual prescribed burning has limited shrub encroachment (Wedel and others 2024). Previous research at this site provides evidence that shrubs can increase the abundance and depth of coarse roots, enhance soil porosity and saturated hydraulic conductivity, and promote deeper infiltration and drainage of precipitation compared to grasses (Jarecke and others 2024). While increased shrub cover can result in deeper water flow paths and faster flow velocities, we hypothesized that catchments with greater shrub cover would also exhibit greater soil-moisture losses, driven by the deeper rooting systems and increased rates of water uptake by shrubs compared to grasses. We discuss how the rooting systems of woody plants and their capacity to deplete soil water in deep subsurface soil volumes may impact hydrological and biogeochemical cycling in grasslands undergoing woody encroachment.

Materials and Methods

Study Area

Our study took place at the Konza Prairie Biological Station, a 3487-ha native tallgrass prairie in Kansas, USA (Figure 1). The climate in this region is midcontinental with cool, dry winters and warm, wet summers. Most of the precipitation occurs as rainfall between April and September. The mean annual water-year precipitation at the Konza Prairie between 1984 and 2023 was 844 mm, and the mean annual temperature was 12.8°C.

The bedrock at the Konza Prairie consists of merokarst, comprising interbedded limestone and thicker mudstone units. These limestone layers give rise to bench-and-slope landforms, with an elevation difference of roughly 60 m between the ridgetops and the catchment outlets (Sullivan and others 2019). Soils range from 20 to 50 cm deep on the ridgetops to over 2 m deep in valley bottoms (Sullivan and others 2020). Soil properties, including soil texture, bulk density, field capacity, and residual water content (Table S2) were measured at the backslope hillslope position in the grassland site in watershed N1B and woody-encroached site in watershed N4D (Figure 1). Soil analysis methods are described in Jarecke and others (2024). Soil texture at the grass site was silty clay loam in the A horizon (0–25 cm) and clay loam in the B horizons (30–100 cm). The woody-encroached site had greater clay content in both A and B horizons resulting in a soil texture classification of clay loam in the A horizon (0–20 cm) and clay in B horizon (20–75 cm). Soils at the neutron probe sites in watersheds 1D, 4B, and 20B are classified as mesic lowland soils (Pachic Argiustolls, Tully series) characterized by deeper colluvial and alluvial deposits (Craine and Nippert 2014).

The vegetation at the Konza Prairie includes perennial C_4 grasses and a diverse range of C_3 grasses, forbs, and woody plants. Woody encroachment occurs due to a combination of factors including climate warming, rising atmospheric carbon dioxide concentrations, and fire suppression, all of which favor the recruitment and growth of woody species (Briggs and others 2005; Archer and others 2017; Collins and others 2021). Woody shrubs have expanded rapidly across mesic tallgrass prairie since 2000, and shrub cover is particularly pronounced in areas that experienced less-frequent prescribed fire (Ratajczak and others 2014). Among the woody plant species encroaching at the Konza Prairie, *Cornus drummondii* (rough-leaf dogwood) is the most prevalent. Other encroaching woody species include *Rhus glabra, Rhus aromatica, Gleditsia triacanthos, Juniperus virginiana, Prunus americana, Zanthoxylum americanum, and Rubus pensilvanicus* (Wedel and others 2024). In 1984, vegetation was the same across neutron probe sites and dominated by perennial warm-season grasses, primarily *Andropogon gerardii*, *Sorghastrum nutans*, and *Schizachyrium scoparium*. Other graminoids and perennial forbs were present with high species diversity but low abundance (Craine and Nippert 2014).

The Konza Prairie is divided into 60 watersheds that are managed with different prescribed fire frequency (burned every 1, 2, 4, or 20 years) and

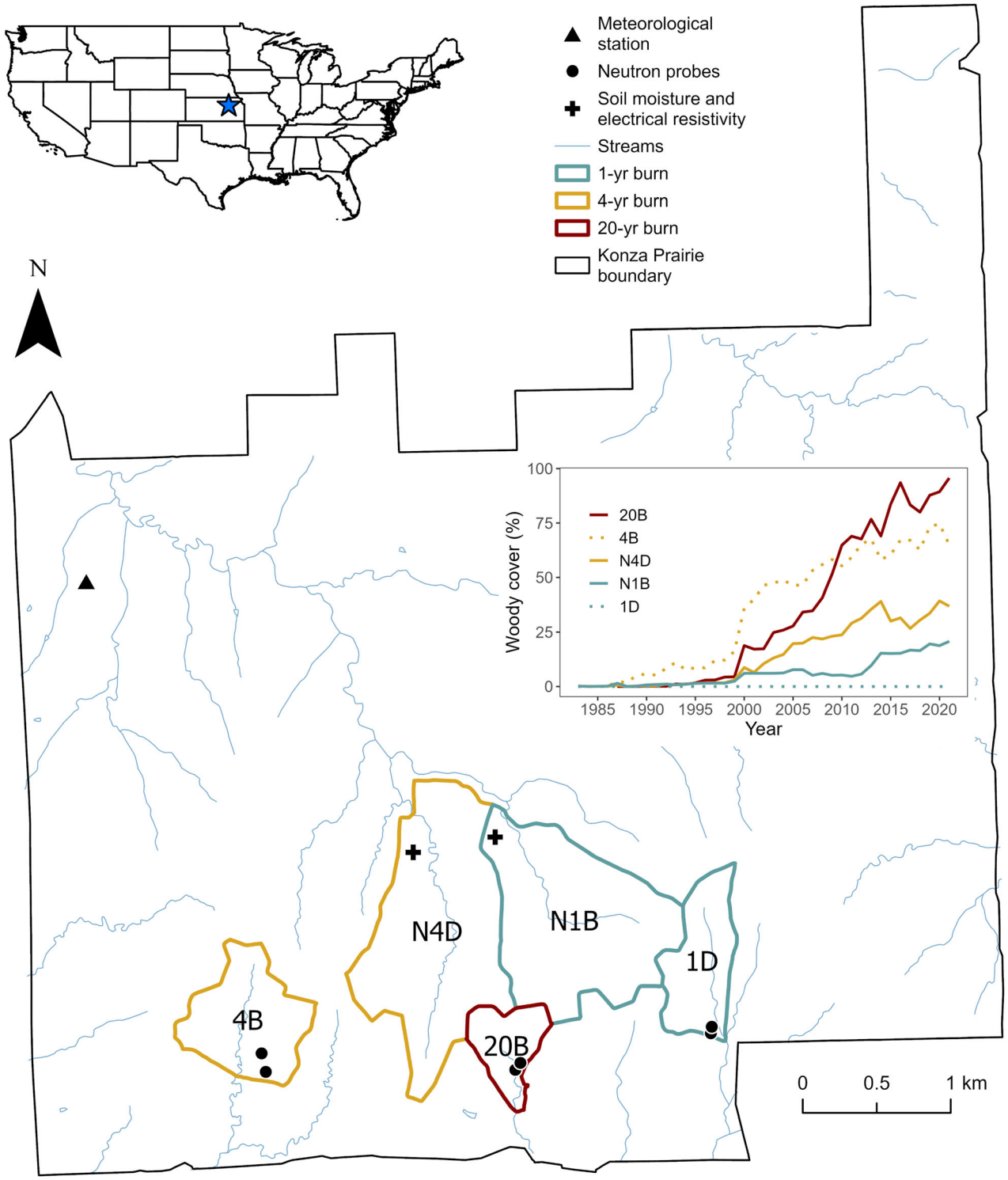

Figure 1. The Konza Prairie is located in Kansas, USA. Precipitation, air temperature, and relative humidity were recorded at the Konza Prairie headquarters' meteorological station. We used measurements from neutron probes (1984–2021) in watershed 1D, 4B, and 20B (points). In addition, we used soil sensors (2021–2024) and electrical resistivity surveys (2022) in watersheds N1B and N4D (crosses) to assess soil moisture at different temporal and spatial scales. Watersheds 1D and N1B underwent prescribed burns annually to prevent increases in woody encroachment. A slight increase in the cover of dominant woody encroachers occurred in N1B but not 1D from 1983 to 2021. Woody cover increased moderately in watersheds 4B and N4D (burned every four years), while watershed 20B (burned every 20 years) saw the greatest increase.

grazing treatments (grazed by American bison or ungrazed). Table 1 details the fire and grazing treatments for the watersheds included in this study. Watersheds 1D and N1B were burned every spring. There was no increase in woody cover in the ungrazed watershed 1D between 1983 and 2021. However, the cover of dominant woody encroachers in the grazed watershed N1B increased from 0.2% in 1983 to 21% by 2021 (Figure 1) because grazing reduced C_4 grass dominance, allowing forbs and shrubs to increase their cover (Collins and others 1998; Veen and others 2008; Ratajczak and others 2022). However, this increase was modest compared to watersheds burned less frequently. We refer to 1D and N1B as '1-yr burn' watersheds. Greater woody cover expansion occurred in watersheds burned every four years, 4B and N4D, which we refer to as '4-yr burn' watersheds. The largest increase in woody cover was observed in the 20-yr burn watershed 20B, where prescribed fires were implemented every 20 years. This watershed was the most severely encroached—woody cover reached 96% by 2021, compared to just 0.03% in 1987 (Figure 1).

Meteorological and Soil-Sensor Data

Precipitation, air temperature, and relative humidity were measured every 15 min at the Konza Prairie Headquarters (Figure 1). Precipitation was collected with an OTT Pluvio^2 rain gauge (OTT HydroMet). Air temperature and relative humidity were collected with an HMP5C probe (Campbell Scientific, Inc.). Soil moisture, soil temperature, and electrical resistivity (ER) were measured at the midslope position in N4D (woody-encroached) and N1B (non-encroached). Three soil sensors were installed in November 2020 at each of three soil depths (15, 40, and 60 cm) beneath *Cornus drummondii* (rough-leaf dogwood) in N4D and beneath grasses in N1B. Soil moisture and soil temperature were recorded every 30 min after installing frequency-domain reflectometry sensors (TEROS-12, METER, Pullman, WA, USA) horizontally into undisturbed soil. We used soil moisture and precipitation time-series data over approximately 3.3 years—April 1, 2021, to July 21, 2024 (Figure 2). Large gaps of missing data occurred in N1B between May 10, 2023, and August 21, 2023, due to power issues to the data logger. Thus, we excluded data during this period from our analysis. Soil oxygen was also recorded every 30 min at the same soil depths as soil moisture. We calibrated the millivolt output of each soil O_2 sensor (SO-120, Apogee Instruments, Logan, UT, USA) in open air at 100% humidity prior to deployment. The sensors were then installed horizontally, less than 30 cm from the adjacent soil-moisture sensors.

Event Drying Analysis

We used soil-moisture measurements from frequency-domain sensors described above to quantify soil drying following individual storm events. Measurements at 15 and 60 cm depths were used to quantify relatively shallow and deep soil drying. However, we acknowledge that limited spatial replication may not fully capture underlying heterogeneity in subsurface moisture dynamics.

We delineated storms and identified the peak soil moisture during each storm following the methods described in Jarecke and others (2024). The decline in soil moisture after the peak was examined for individual storm events. Soil-drying periods ended at the minimum soil-moisture value that occurred

Table 1. Descriptions of Subsurface Measurements, Watershed Size, Burn Frequency, and Grazing Treatments in Each of the Study Watersheds—N1B, N4D, 1D, 4B, and 20B.

	Measurements	Watershed size (ha)	Burn frequency	Grazing treatment
N1B	Soil moisture Soil temperature ERT	120.9	1-yr	Grazed
N4D	Soil moisture Soil temperature ERT	135.7	4-yr	Grazed
1D	Neutron probe	41.6	1-yr	Ungrazed
4B	Neutron probe	54.2	4-yr	Ungrazed
20B	Neutron probe	58.7	20-yr	Ungrazed

Figure 2. Daily rainfall and maximum daily vapor pressure deficit (VPD) at the Konza Prairie headquarters and the volumetric soil water content measured every 30 min at soil depths of 15 and 60 cm from April 1, 2021 to July 21, 2024. The grass site is located in watershed N1B and the woody-encroached site is located in N4D. The growing season from April to September coincides with elevated VPD, larger rainfall events, and increased soil-moisture variability than the dormant season from October to March.

before the next soil-moisture peak. We excluded drying periods that lasted less than 2 days and more than 60 days as well as periods that contained two or more consecutive hours of missing data. Drying periods were also excluded from further analysis if the maximum soil-moisture value was below the field capacity or if the minimum soil-moisture value was above the field capacity. These criteria enabled us to isolate drying curves that included both soil-moisture decline caused by gravity drainage and decline due to evapotranspiration (ET). After gravity drainage, downward unsaturated flow occurs but at a much smaller rate than ET. We estimated unsaturated hydraulic conductivity to be less than 0.1 mm day^{-1} for soils at our site (data not shown), compared to canopy transpiration rates of approximately 0.91 mm day^{-1} from dominant grasses (*A. gerardii*) and 2.01 mm day^{-1} from dominant shrubs (*C. drummondii*) at the Konza Prairie (O'Keefe and others 2020). Therefore, we attribute post-drainage soil moisture declines primarily to ET. Finally, we removed drying periods when the overall soil-moisture decline was less than 0.03 m^3 m^{-3}, which is the accuracy limit of our soil-moisture sensors.

Next, we isolated the portion of each drying period where drying occurred due to ET and followed rapid gravity drainage. To do this, we found the minimum first derivative of the locally estimated scatterplot smoothed (LOESS) volumetric water content (dVWC/dt) for the entire drying period (Figure 3). The minimum first derivative occurred when soil moisture declined rapidly due to drainage, which occurred, on average, within 32 h of the onset of soil drying. We then identified the time stamp after the minimum derivative value when the derivative became greater than $-$ 0.01 m^3 m^{-3}. We chose this value after testing multiple values ranging from $-$ 0.03 to $-$ 0.005 and visually inspected drying curves to identify the

value that captured the shift from relatively steep declines in soil moisture (more negative derivatives) to gentler declines (less negative derivatives), which we interpreted as the transition from rapid drainage to slower ET drying. We visually assessed whether soil moisture declines above and below field capacity captured the transition from rapid gravity drainage to slower unsaturated drying, but we found this method to be highly inconsistent, leading to over- or underestimates in the timing of ET drying. Thus, we concluded that the derivative-based approach more accurately captured this transition.

Seasonal Drying Analysis

We quantified the change in electrical resistivity (ER) between June 29 and October 3, 2022, which spans the warmest period of the year. The change in ER between the two dates allowed us to determine how soil drying over the growing season differed below grass and roughleaf dogwood over a broader spatial extent than the soil-moisture probes. There was 119 mm of rainfall during the two weeks prior to the June sampling date and 18 mm of rainfall during the two weeks prior to the October sampling date. The ER transects were established in watersheds N1B and N4D (Figure 1) ~ 5 m upslope of our soil-moisture sensors in the mid-hillslope position. The transect in N1B was covered by grasses including big bluestem (*Andropogon gerardii*), switchgrass (*Sorghastrum nutans*), and Indiangrass (*Panicum virgatum*) as well as forbs—Baldwin's ironweed (*Vernonia baldwinii*), white sagebrush, (*Artemisia ludoviciana*), Canada goldenrod (*Solidago canadensis*), and butterfly milkweed (*Asclepias tuberosa*). The transect in N4D was centered on a transition from a similar species composition of grasses and forbs to roughleaf dogwood (*Cornus drumondii*).

Each transect was 22.5 m and ran north to south with relatively little change in elevation. We installed 46 electrodes spaced every 0.5 m along each transect and monitored soil ER using a ZZ Universal 96 resistivity unit (ZZ Resistivity Imaging, South Australia). ER data sets were collected using a dipole–dipole configuration. We collected three data sets on each sampling date and 316 quadripoles per data set. We used the mean of apparent resistivity from the three data sets in the inversion. We then corrected the mean apparent resistivity values for differences in mean soil profile temperature between the June and October survey dates using Hayley and others (2007). The mean daily soil profile temperature was calculated from 30-min measurements at 15, 45, and 60 cm. Soil temperature was assumed to be laterally uniform at each site and differences beneath each land cover were

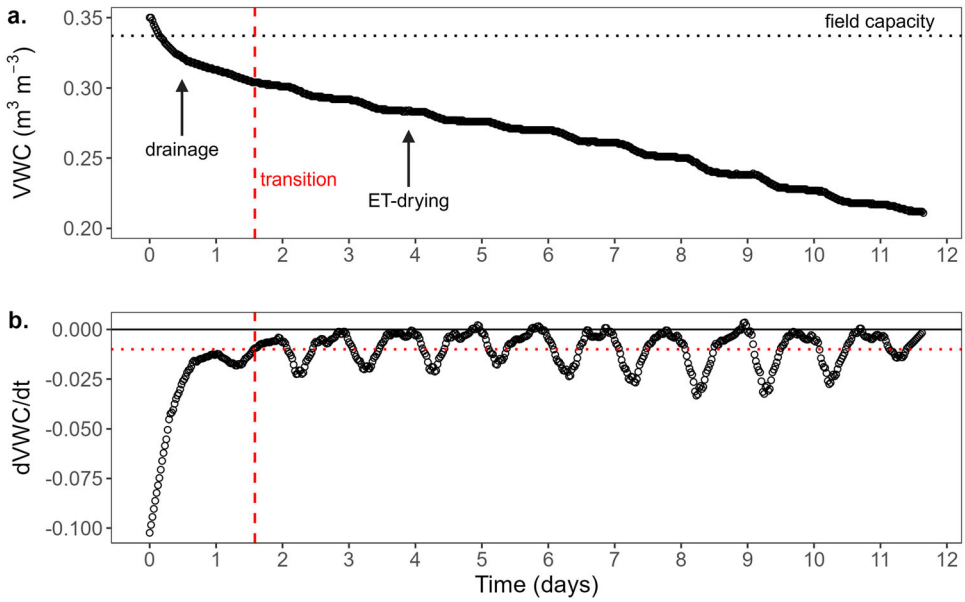

Figure 3. Example of a soil-moisture drying period following a storm event, showing (**a**) the transition from drainage to evapotranspiration (ET)-driven drying marked by the vertical dashed red line. (**b**) We identified ET drying when the first derivative of the loess-smoothed soil moisture (dVWC/dt) first reached a value greater than − 0.01 (horizontal dotted red line) after the onset of drying. Soil drying periods ended at the minimum soil-moisture value that occurred before the next soil-moisture peak.

assumed to be negligible beneath 60 cm based on the minimal changes in soil temperature at 60 cm.

We inverted the temperature-corrected data using ResIPy v3.5.4 (Blanchy and others 2020). The standard deviation of repeat measurements from the three datasets on each sampling date were used to weight the data in the difference inversion. The median standard deviation in June was 0.001 Ω-m at the grass transect and 0.002 Ω-m at the woody-encroached transect. The median standard deviation in October was 0.005 Ω-m at the grass transect and 0.009 Ω-m at the woody-encroached transect. Linear filtering was used to regularize the difference inversion for estimating change in resistivity (LaBrecque and Yang, 2001). We used the depth of investigation method (Oldenburg and Li 1999) within the ResIPy software to estimate the depth below which the model was minimally sensitive to the data in our background data set. Inversions generally were sensitive up to 2 m deep beneath the woody-encroached transect and up to 2.5 m beneath the grass transect. A positive change in resistivity from the time-lapse inversions indicated an increase in resistivity from the background data (June 2022), which was used as a proxy for examining the spatial patterns of soil drying from June to October 2022.

Decadal Drying Analysis

Neutron probe data were available from 1984 to 2021 (Nippert 2024). Soil-moisture measurements were taken at 25, 50, 75, 100, 125, 150, 175, and 200 cm and reported in units of kg m^{-3}. We excluded the 200 cm depth from our analysis due to substantial periods of missing data. At two times within this record, the model of probe used for measurements was changed (January 1998 and December 2015, Figure S1). A Troxler 3400 (Troxler Electronic Laboratories, NC, USA) was used from 1984 to 1998, a Troxler 4300 was used from 1998 to 2015, and an InstroTek CPN 503 (InstroTek Inc., NC, USA) was used from 2015 to 2021. We selected watersheds 1D (1-yr burn), 4B (4-yr burn), and 20B (20-yr burn; Table 1) for these analyses because all three have complete records. We chose not to use the grazed replicates (N1B, N4D, N20B) because the record for the grazed 1-yr burn watershed (N1B) ended in 1992 and was needed to compare to the less frequently burned watersheds with higher woody cover. Burn treatments were initiated in these watersheds between 1977 and 1983, and substantial increases in woody cover in less frequently burned watersheds were mainly observed after 2000 (Figure 1, Ratajczak and others 2014).

Each watershed had two permanent access tubes for neutron probe measurements (Figure 1), and measurements were taken every two weeks from April to November, and then once per month from November to March when temperatures were above − 6.6°C. For each watershed, we averaged the values from the two access tubes prior to analysis. We calculated z-scores and values greater than 2.5 standard deviations from the mean were considered outliers and removed (Figure S1). Values removed as outliers comprised less than 1% of total data points. After removing the outliers, we calculated the difference in mean annual soil-moisture values between the 1-yr burn watershed and the 4-yr and 20-yr burn watersheds:

$$\Delta SM_{4-yr\ burn} = SM_{1-yr\ burn} - SM_{4-yr\ burn},$$

$$\Delta SM_{20-yr\ burn} = SM_{1-yr\ burn} - SM_{20-yr\ burn}$$

where $SM_{1\text{-yr burn}}$, $SM_{4\text{-yr burn}}$, and $SM_{20\text{-yr burn}}$ represent annual mean soil-moisture values for the non-encroached (1D), moderately encroached (4B), and severely encroached (20B) watersheds, respectively. These differences were calculated to examine drying in the encroached watersheds relative to the non-encroached watershed to avoid comparing raw moisture values and any issues caused by the probe switches in 1998 and 2015.

Linear regression and modified Mann–Kendall tests with trend-free pre-whitening (Mann 1945; Kendall 1948) were performed using the *tfpwmk* function in the *modifiedmk* package in R (Patakamuri and O'Brien 2021) for each depth and treatment combination separately. We gap-filled missing mean annual soil-moisture values at the 175 cm depth using time-series spline interpolation with the *na.interp* function from the *forecast* package in R (Hyndman and others 2020) before performing the Mann–Kendall test because Mann–Kendall trends tests cannot handle missing values. For both treatment comparisons (1-yr vs. 4-yr and 1-yr vs. 20-yr), 18% (seven of 39 total years) of data was missing and needed to be interpolated. Shallower depths (25, 50, 75, 100, 125, and 150 cm) did not have missing values to gap fill.

Results

Event Drying

We observed a greater number of soil-drying periods at the grass site in N1B compared to the woody-encroached site in N4D (Figure S2). Specifically, at

15 cm depth, there were 46 drying periods beneath grasses and 29 beneath shrubs, while at 60 cm, we identified 20 drying periods beneath grasses and 10 beneath shrubs. Before the onset of ET drying, rapid soil drainage occurred (for example, Figure 3). Soil drainage lasted, on average, 23 h beneath grasses (SD = 11 h) and 32 h beneath shrubs (SD = 18 h). Higher clay content at the woody-encroached site compared to the grass site (Table S1) may contribute to slower drainage at that location.

The impact of vegetation type on soil-moisture dynamics revealed greater soil-moisture decline beneath shrubs than grasses at 60 cm but not at 15 cm. Following the onset of ET drying, the average duration of a drying period at 15 cm was 9 d (SD = 8 d) beneath both grasses and shrubs. The average total soil-moisture decline between 1 and 18 d was similar beneath both vegetation types at 15 cm (Figure 4). However, for drying periods that lasted up to 22 d, the average total decline was 8.7% greater beneath shrubs compared to grasses. The length of drying periods lasted longer at 60 cm compared to 15 cm, averaging 16 d (SD = 13 d) beneath grasses and 19 d (SD = 13 d) beneath shrubs. We found that total soil-moisture decline at 60 cm was more pronounced beneath shrubs than grasses after $\sim$ 7 d of drying (Figure 4). The average decline in soil water content was 4–13% greater beneath shrubs than grasses for drying periods that lasted between 7 and 34 d and was 14–20% greater beneath shrubs for events that lasted between 34 and 42 d (Figure 4).

Due to the difference in the number of drying periods between the grass and shrub sites (Figure S2), we also repeated our analysis and included only storm events where both the grass and shrub sites had a drying signal. If a drying period occurred after a storm at the grass site but not the woody-encroached site or vice versa, it was not included in the analysis. As a result, there were fewer drying periods captured at 15 cm and 60 cm than in our original analysis. There were 17 drying periods at 15 cm and 4 events at 60 cm in which both the grass and shrub sites responded to the same storm event. Despite this reduced sample size, the average decline in soil moisture at 15 cm beneath the grass and shrubs was similar to our results that included all storm events (Figure S3). However, at 60 cm depth, soil moisture declined 3–12% more beneath shrubs than grasses during drying periods lasting 7–34 days (Figure S3).

Seasonal Drying

Time-lapse ER imaging revealed soil drying between June and October below the woody-encroached transect in N4D and grass transects in N1B. An increase in resistivity was used as a proxy for soil water decrease from June 29 to October 3, 2022. The percentage change in resistivity was positive in the upper 2 m of soil beneath the ER transects, reflecting drier soil conditions in October compared to June. There was a greater increase in soil drying (greater percent change in resistivity) in the upper 2 m at the woody-encroached transect (Figure 5a) compared to the grass transect (Figure 5b). The mean increase in resistivity for the upper 2 m was 1.6 times greater beneath the woody-encroached transect (441%) compared to beneath the grass transect (271%). Along the transect, change in resistivity was most variable in the upper 0.5 m (Figure S4). However, the greater increase in resistivity at the woody-encroached compared to the grass site was notable across the depth profile, with the greatest differences occurring between 1 and 2 m (Figure S4).

Decadal Drying

The difference in mean annual soil moisture between the 1-yr burn watershed (1D) and the 4-yr burn (4B) and 20-yr burn (20B) watersheds showed a positive linear trend from 1984 to 2021 (Figure 6). This indicated an increasing degree of soil drying over time in the more encroached (4- and 20-yr burn) watersheds compared to the non-encroached (1-yr burn) watershed. Sen's slopes for this trend were statistically significant (p value ranged from 0.01 to < 0.001) at all soil depths for the 1-yr burn vs. 20-yr burn comparison, and at all but the 25 and 50 cm depths for the 1-yr burn vs. 4-yr burn comparison (p value ranged from 0.003 to < 0.001, Table S2).

The slopes were greater for deeper soils (75–150 cm) compared to shallower soils (25–50 cm) and were highest at the deepest measured depth of 175 cm, indicating a stronger drying trend in deeper soil layers (Figure 6, S5, S6). Additionally, slope values for the 1-yr burn vs. 20-yr burn comparison exceeded those for the 1-yr burn vs. 4-yr burn comparison at all depths except 120 cm (Table S2), suggesting a more pronounced drying trend in the watershed with the greatest amount of woody cover.

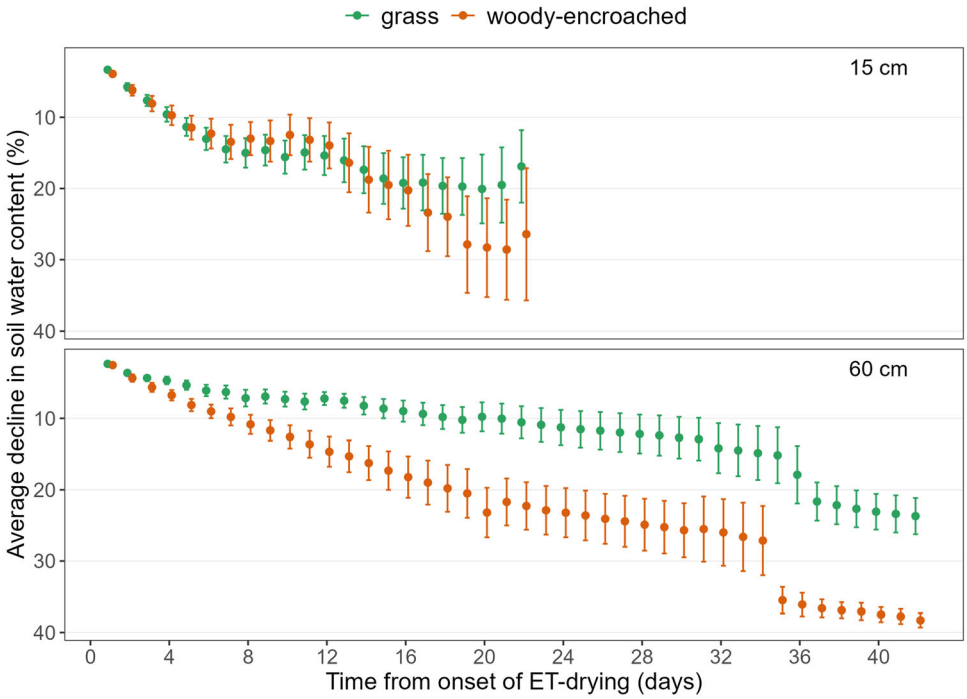

Figure 4. The average decline in soil moisture (%) at 15 cm and 60 cm beneath grasses and shrubs (woody-encroached). Points represent mean values across all drying periods, with error bars indicating ± standard error. We isolated the portion of each drying period that began after soil drainage ended, during which further declines in soil moisture were primarily driven by evapotranspiration (ET). The percent decline in soil moisture is relative to the soil moisture at the onset of ET drying. There was a greater decline in soil moisture beneath shrubs than grasses at 60 cm but not at 15 cm.

Discussion

Woody Encroachment Intensifies Deep Soil Drying

Our findings suggest deep soil drying is exacerbated in woody-encroached areas over timescales ranging from days to decades. Increased soil drying beneath shrubs was most pronounced at intermediate-to-deep soil depths (50–200 cm) compared to near-surface soils (< 50 cm) over all temporal scales. Initial analyses of soil-moisture trends at the Konza Prairie between 2002 and 2010 showed that shrub expansion was associated with greater soil-moisture losses in deep soils (75–125 cm) but not in shallow soils (25 and 50 cm; Craine and Nippert, 2014). Our analysis of long-term neutron probe data supports these findings and extends our understanding of the scope of long-term, continued decline in soil moisture in woody-encroached catchments. For instance, the positive linear trends in Figure 6 suggest that the amount of soil moisture depletion from deep soils is increasing due to the progressive expansion of woody plants in areas with low burn frequency. Notably, more intense soil drying occurred in the 20-yr burn watershed compared to the 4-yr burn watershed. Interestingly, both the 4-yr and 20-yr burn watersheds started out wetter in deeper soil layers than the annually burned watershed potentially due to heterogeneity in subsurface properties. Despite this, soil moisture was lower in the 4-yr and 20-yr burn watersheds by the end of the long-term soil moisture record in 2020 (Figure 6), highlighting the strong drying trends in areas with increased woody cover.

The intensification of soil drying that has occurred over decades in woody-encroached grasslands is consistent with, and thus likely driven by, the water use strategies of encroaching shrubs and trees (Keen and others 2024a, 2024b; Zou and others 2018) that allow them to maintain higher canopy transpiration rates compared to grasses even when shallow soil water availability becomes limiting (O'Keefe and others 2020). While C_4 grasses of tallgrass prairie can have rooting depths up to 2 m, total root biomass and water uptake are concentrated in shallow (< 30 cm) soil layers (Nippert and others 2012; Nippert and Knapp 2007). Results from isotopic studies at the Konza Prairie suggest that encroaching shrubs take up surface soil moisture during wetter periods of the growing season but shift to deeper soil moisture

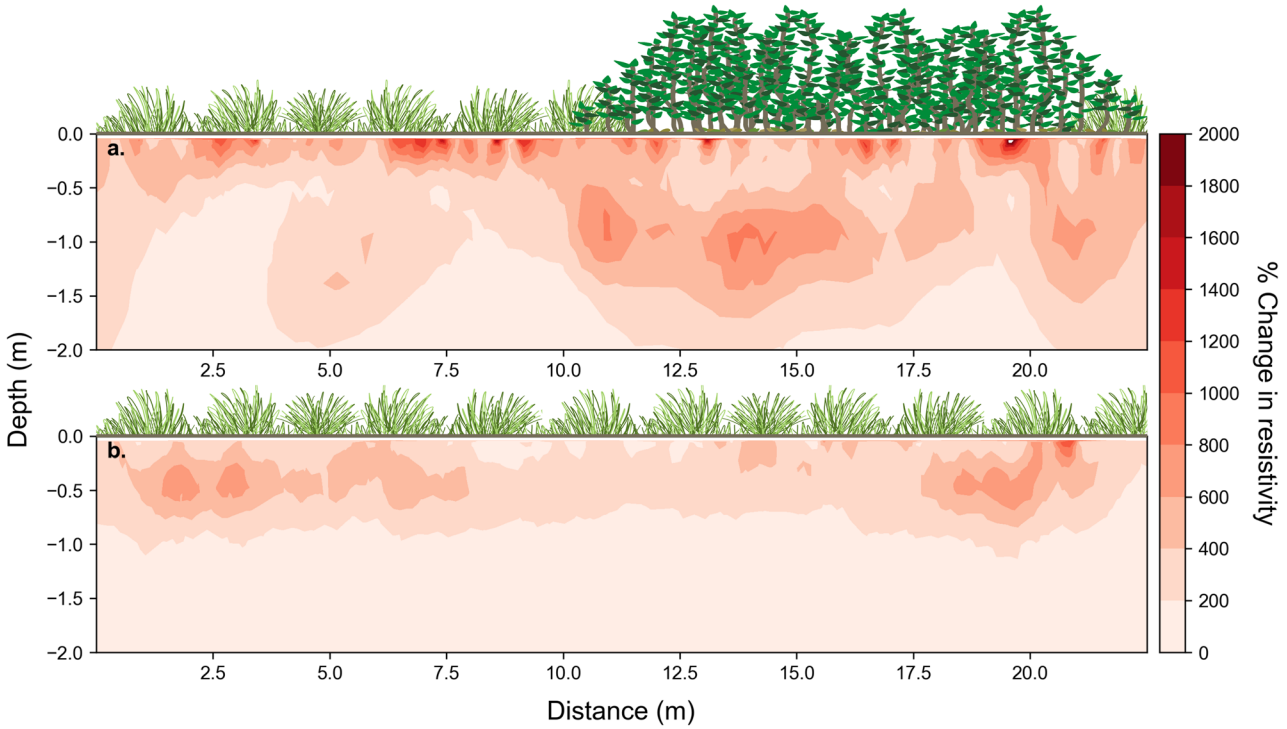

Figure 5. Change in ER from June 29 to October 3, 2022 at the (**a**) woody-encroached (N4D) and (**b**) grass transects (N1B). An increase in the inverted resistivity indicates a decrease in soil moisture. The upper 2 m of the woody-encroached transect exhibited a larger increase in soil drying (higher percent change in resistivity) compared to the grass transect.

when water becomes limiting (Keen and others 2024a, 2024b), thus avoiding direct competition with C_4 grasses during drier periods of the growing season. At this site, soil water $\delta^{18}O$ declines with depth but levels off between 40 and 60 cm (Nippert and Knapp 2007). As a result, isotopic studies are limited to assessing plant water uptake up to 60 cm. Drying in deeper soil layers (50–200 cm) indicates that water uptake by clonal shrubs extends deeper into the soil profile than can be measured with isotopes alone.

Our results agree with other studies that report that woody shrubs and trees use deeper water sources than neighboring grasses, especially during seasonally dry periods (Acharya and others 2017a, 2017b; Jayawickreme and others 2008; Kulmatiski and Beard 2013a; Niemeyer and others 2017; Zou and others 2014). Moreover, our inferences are consistent across multiple spatial and temporal scales. In addition to greater seasonal and annual drying, our analysis of soil-moisture declines between storm events suggest that shrubs use a greater proportion of deep soil moisture than grasses over relatively short time scales—for example, days to weeks (Figure 4). These results suggest that shrubs use water from deeper soil horizons, even without significant water stress. Soil-moisture dynamics differed beneath the grasses and shrubs such that very few storms (n = 4) were followed by concurrent drying periods at 60 cm beneath both shrubs and grasses. This limited our ability to compare drying rates across a full range of antecedent conditions. A longer record of high-frequency soil-moisture data could help to clarify how soil drying rates respond to differences in antecedent soil moisture and atmospheric vapor pressure deficit. In addition, differences in initial moisture conditions—potentially due to variations in soil properties and subsurface flow beneath shrubs and grasses—may have influenced the magnitude of seasonal soil drying observed by electrical resistivity measurements.

The intensification of soil drying due to woody encroachment is of particular interest given that movement of water to deeper soil depths can also occur with shrub or tree encroachment (Kulmatiski and Beard 2013b; Jarecke and others 2024). In a mesic grassland site in Oklahoma, USA, the encroachment of eastern red cedar increased infiltration capacity of the soil (Zou and others 2014); however, a large portion of this water was used by woody plants, and as a result, the downward flux

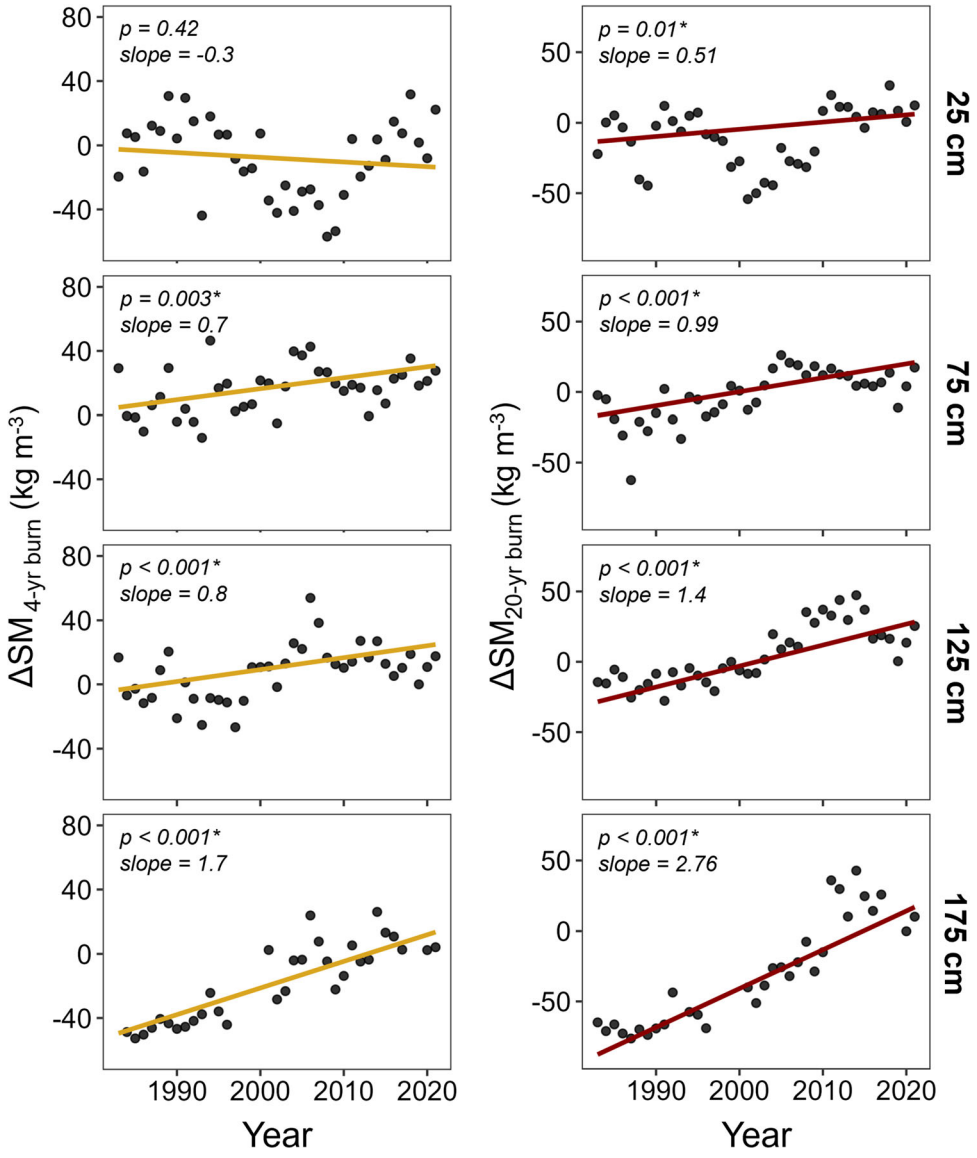

Figure 6. Difference in mean annual soil moisture at 25, 75, 125, and 175 cm between the 1-yr burn and 4-yr burn watersheds ($\Delta SM_{4\text{-yr burn}}$) and between the 1-yr burn and 20-yr burn watersheds ($\Delta SM_{20\text{-yr burn}}$) from 1984 to 2021; *p* values correspond to the modified Mann–Kendall test and the slope refers to the Sen's slope value. Negative values indicate the moisture content at the 1-yr burn watershed was less than that of the 4-yr and 20-yr burn watersheds while positive values indicate the opposite.

of water below the rooting zone decreased (Acharya and others 2017a, 2017b). The deep soil drying trends in this study support the idea that, although woody root systems can increase infiltration depths in the hours immediately following rain events (Jarecke and others 2024), the net effect of shrub encroachment over longer timescales is soil drying, and ultimately, declines in water yield (Sadayappan and others 2023; Keen and others 2024a, 2024b). These competing processes, now evident to varying degrees at multiple sites, highlight the challenges of predicting the net consequences of woody encroachment on deep soil-moisture variations.

Moisture Whiplash Induced by Woody Encroachment May Have Strong Implications for Deep Biogeochemical Processes

In grasslands, soil moisture typically fluctuates less in deep soils compared to near-surface soils, where rainfall infiltration and plant water uptake are more dynamic. However, changes in rainfall

patterns and the deepening of woody root systems could potentially alter the magnitude and frequency of wet-dry cycles in deep soil layers. In this context, we define 'moisture whiplash' as the rapid shift from extremely dry to very wet soil conditions. Similar terms, including 'weather whiplash' and 'hydroclimate whiplash', have been used to describe the abrupt transition from extremely dry to wet meteorological conditions (Swain and others 2025). Research indicates that such transitions have increased globally from 1940 to 2023, driven by rising evaporative demand and the atmosphere's increasing water–vapor-holding capacity (Swain and others 2025).

Climate-change projections for the central United States predict an increase in the frequency and severity of growing season drought, in addition to more frequent and intense extreme precipitation events (Easterling and others 2000; Hatfield and others 2013; Flanagan and Mahmood 2021). The Great Plains region in particular is a hotspot for the rapid intensification of droughts, known as 'flash droughts', which have increased in frequency from 1979 to 2016 due to rising temperatures and increased evaporative demand (Christian and others 2019). Observations from the Konza Prairie (1898 to 2021; Keen and others 2024a, 2024b) and across the central Great Plains (1979 to 2013; Feng and others 2016) have also shown that large rainfall events are becoming more frequent in this region. The juxtaposition of more frequent flash droughts with an increase in large rainfall events highlights the region's growing susceptibility to extreme hydrological variability. These conditions are expected to favor deeply rooted woody plants by directing more water to deeper soil layers that are more accessible to shrubs and trees than grasses (Kulmatiski and Beard 2013b). Enhanced preferential flow to deeper soil layers that can occur with increased rainfall intensity and/or prolonged rainfall (Hu and others 2019) may be even more exaggerated where soils are rich in 2:1 clay minerals, such as those at our study site. These soils can exhibit considerable shrinking of soil structural units under dry conditions, which can significantly increase soil macroporosity (Hirmas and others 2025) and enhance the occurrence of preferential flow (Demand and others 2019).

Changes to soil-moisture variation, including moisture whiplash events, will have important implications for biogeochemical processes. For example, soil-moisture variations strongly affect soil O_2 concentrations, and thus the overall rate of respiration as well as proportions of anaerobic and aerobic respiration (Tiedje and others 1984). Time-series data of soil O_2 concentrations at our site also revealed that gas exchange with the atmosphere occurred more readily beneath shrubs than grasses at 60 cm (Figure 7). The variation in soil O_2 concentrations, particularly in 2022 and 2024, demonstrates the enhanced ability of woody-encroached soils to rapidly restore atmospheric O_2 after a rainfall event. The more rapid re-supply of soil O_2 after periods of O_2 depletion beneath shrubs may be the result of the coarser root abundance beneath shrubs compared to grasses (Jarecke and others 2024). Root coarsening in woody-encroached soils can increase the abundance of soil macropores, which in turn may increase the efficiency of gas exchange between the soil and atmosphere (Hinsinger and others 2009; Wen and others 2022). As a result, processes that modify soil-moisture dynamics deep within the soil profile by altering root abundance and size have the potential to shift soil gas fluxes and associated O_2 availability, and thus the redox conditions that govern soil microbial activities (Billings and others 2024). Furthermore, the rewetting of relatively dry soils, compared to those with high antecedent moisture contents, can significantly increase soil respiration rates leading to greater soil emission of CO_2 (Tiemann and Billings 2011; Sang and others 2022).

While drier conditions promote the vertical transport of soil CO_2 to the atmosphere (Wen and others 2022), relatively wet conditions, especially after a period of drought, can increase the mobilization of dissolved organic carbon (Kaiser and Kalbitz 2012; Bowering and others 2023; Souza and others 2023). Radiocarbon data from across the Midwest US suggest that rapid water penetration can deliver fresh photosynthate deep into the soil profile (Souza and others 2023). This suggests that deep carbon accumulation could accompany shrub encroachment from surface- or near-surface dissolved organic carbon infiltrating preferential flow paths to deep horizons. In addition, woody encroachment may promote carbon accumulation through input of root-derived soil organic carbon into deep soil (Li and others 2019), where soil organic carbon pools have a greater probability of long-term storage (Hicks Pries and others 2023).

Conclusion

Soil moisture is a key driver of water and carbon cycling in grassland ecosystems. Our results show that woody encroachment in a mesic grassland intensified soil drying from event to seasonal to decadal scales. This effect is more pronounced in

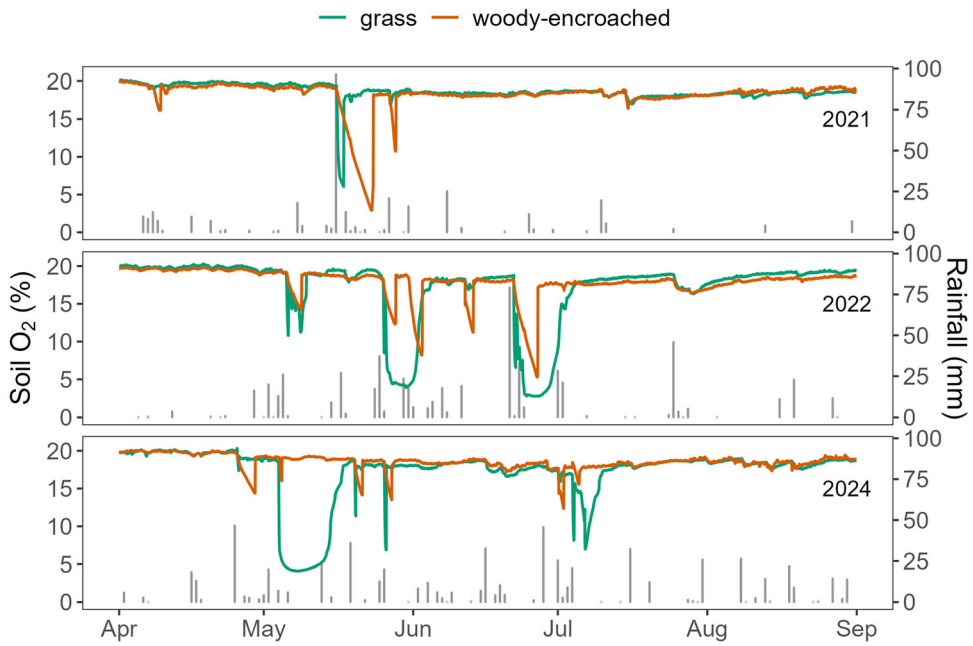

Figure 7. Daily rainfall from Konza Prairie headquarters and hourly soil oxygen concentrations at 60 cm at the grass (N1B) and woody-encroached (N4D) sites during the growing season (April to September) in 2021, 2022, 2024. We did not include the 2023 growing season since 60% of data were missing due to data logger failure.

deeper soil horizons (50–200 cm) compared to near-surface soils across all timescales. High transpiration rates and the ability of shrubs to shift to deeper water sources have exacerbated soil drying during more than three decades of rapid shrub expansion. Intensified soil drying is concurrent with observations of increased stream drying despite increases in precipitation in the central Great Plains. As woody encroachment in grasslands continues, shifting climate conditions—marked by extreme drought and heavy rainfall—are likely to amplify subsurface moisture variations in deep soil layers, with significant implications for grassland carbon and nutrient cycling.

ACKNOWLEDGEMENTS

We thank Victoria Moreno, Keira Johnson, and Josiah Chan for assistance with the installation and maintenance of soil sensors. We thank Yang Xia and Jeff Taylor for maintaining the long-term data collected at the Konza Prairie. Any opinions, findings, and conclusions or recommendations expressed in this material are those of the authors and do not necessarily reflect the views of the National Science Foundation.

FUNDING

Our funding was supported by the National Science Foundation (NSF 2121694 [PLS]; 2121659 [KS]; 2024388 [PLS]; 2121652 [JBN]; 1911969 [JBN]; 2121760 [HA, DRH]; 2034232 [PLS]; 2034214 [LL]; 2121639 [SB]; 2415981[LL]; 2415979 [PLS]; 2415980 [MK, JBN]) and the USDA National Institute of Food and Agriculture (2021-67019-34341 [HA, DRH]; 2021- 67019-34338 [SAB]; 2021-67019-34340 [ANF]).

DATA AVAILABILITY

Data are archived at http://lter.konza.ksu.edu/data (Nippert 2024; Sullivan and Jarecke 2024).

Declarations

Conflict of interest

None.

OPEN ACCESS

REFERENCES

Acharya BS, Halihan T, Zou CB, Will RE. 2017a. Vegetation controls on the spatio-temporal heterogeneity of deep moisture in the unsaturated zone: a hydrogeophysical evaluation. Sci Rep 7:1499.

Acharya BS, Hao Y, Ochsner TE, Zou CB. 2017b. Woody plant encroachment alters soil hydrological properties and reduces downward flux of water in tallgrass prairie. Plant Soil 414:379–391.

Acharya B, Kharel G, Zou C, Wilcox B, Halihan T. 2018. Woody plant encroachment impacts on groundwater recharge: a review. Water 10:1466.

Archer SR, Anderson EM, Predick KI, Schwinning S, Steidl RJ, Woods SR. 2017. Woody plant encroachment: causes and consequences. Rangland systems: processes, management, and challenges, . Springer Series on Environmental Management: Cham. pp 25–84.

Billings SA, Brecheisen Z, Cherkinsky A, Lehmeier C, Cook CW, Markewitz D, Souza LFT, Reuman D, Richter DD. 2024. Persistent biogeochemical signals of land use-driven, deep root losses illuminated by C and O isotopes of soil CO_2 and O_2. Biogeochemistry 167:1469–1489.

Blanchy G, Saneiyan S, Boyd J, McLachlan P, Binley A. 2020. ResIPy, an intuitive open source software for complex geoelectrical inversion/modeling. Comput Geosci 137:104423.

Bowering KL, Edwards KA, Wiersma YF, Billings SA, Warren J, Skinner A, Ziegler SE. 2023. Dissolved organic carbon mobilization across a climate transect of mesic boreal forests is explained by air temperature and snowpack duration. Ecosystems 26:55–71.

Briggs JM, Knapp AK, Blair JM, Heisler JL, Hoch GA, Lett MS, McCarron JK. 2005. An ecosystem in transition: Causes and consequences of the conversion of mesic grassland to shrubland. BioScience 55:243.

Christian JI, Basara JB, Otkin JA, Hunt ED, Wakefield RA, Flanagan PX, Xiao X. 2019. A methodology for flash drought identification: Application of flash drought frequency across the United States. J Hydrometeorol 20:833–846.

Collins SL, Knapp AK, Briggs JM, Blair JM, Steinauer EM. 1998. Modulation of diversity by grazing and mowing in native tallgrass prairie. Science 280:745–747.

Collins SL, Nippert JB, Blair JM, Briggs JM, Blackmore P, Ratajczak Z. 2021. Fire frequency, state change and hysteresis in tallgrass prairie. Comita L, editor. Ecol Lett 24:636–647.

Craine JM, Nippert JB. 2014. Cessation of burning dries soils long term in a tallgrass prairie. Ecosystems 17:54–65.

Demand D, Blume T, Weiler M. 2019. Spatio-temporal relevance and controls of preferential flow at the landscape scale. Hydrol Earth Syst Sci 23:4869–4889.

Deng Y, Li X, Shi F, Hu X. 2021. Woody plant encroachment enhanced global vegetation greening and ecosystem water-use efficiency. Global Ecol Biogeogr 30:2337–2353.

Dodds WK, Ratajczak Z, Keen RM, Nippert JB, Grudzinski B, Veach A, Taylor JH, Kuhl A. 2023. Trajectories and state changes of a grassland stream and riparian zone after a decade of woody vegetation removal. Ecol Appl 33:e2830.

Easterling DR, Meehl GA, Parmesan C, Changnon SA, Karl TR, Mearns LO. 2000. Climate extremes: observations, modeling, and impacts. Science 289:2068–2074.

Feng Z, Leung LR, Hagos S, Houze RA, Burleyson CD, Balaguru K. 2016. More frequent intense and long-lived storms dominate the springtime trend in central US rainfall. Nat Commun 7:13429.

Flanagan P, Mahmood R. 2021. Spatiotemporal analysis of extreme precipitation in the Missouri River Basin from 1950–2019. J Appl Meteorol Climatol 60:811–827.

Guo L, Mount GJ, Hudson S, Lin H, Levia D. 2020. Pairing geophysical techniques improves understanding of the near-surface Critical Zone: visualization of preferential routing of stemflow along coarse roots. Geoderma 357:113953.

Hatfield JL, Cruse RM, Tomer MD. 2013. Convergence of agricultural intensification and climate change in the Midwestern United States: implications for soil and water conservation. Mar Freshwater Res 64:423.

Hayley K, Bentley LR, Gharibi M, Nightingale M. 2007. Low temperature dependence of electrical resistivity: Implications for near surface geophysical monitoring. Geophys Res Lett 34:L18402.

Hicks Pries CE, Ryals R, Zhu B, Min K, Cooper A, Goldsmith S, Pett-Ridge J, Torn M, Berhe AA. 2023. The deep soil organic carbon response to global change. Annu Rev Ecol Evol Syst 54:375–401.

Hinsinger P, Bengough AG, Vetterlein D, Young IM. 2009. Rhizosphere: biophysics, biogeochemistry and ecological relevance. Plant Soil 321:117–152.

Hirmas DR, Ajami H, Sena M, Zhang X, Cao X, Li B, Jarecke KM, Billings SA, Pachon JC, Li L, Nippert JB, Souza LFT, Flores AN, Sullivan PL. 2025. Predicting macroporosity and hydraulic conductivity dynamics: a model for integrating laser-scanned profile imagery with soil moisture sensor data. Waters Resources Research (in press).

Honda EA, Durigan G. 2016. Woody encroachment and its consequences on hydrological processes in the savannah. Phil Trans R Soc B 371:20150313.

Hu H, Wen J, Peng Z, Tian F, Tie Q, Lu Y, Khan MYA. 2019. High-frequency monitoring of the occurrence of preferential flow on hillslopes and its relationship with rainfall features, soil moisture and landscape. Hydrol Sci J 64:1385–1396.

Huxman TE, Wilcox BP, Breshears DD, Scott RL, Snyder KA, Small EE, Hultine K, Pockman WT, Jackson RB. 2005. Ecohydrological implications of woody plant encroachment. Ecology 86:308–319.

Hyndman R, Athanasopoulos G, Bergmeir C, Caceres G, Chhay L, O'Hara-Wild M, Petropoulos F, Razbash S, Wang E, Yasmeen F. 2020. Package 'forecast'. https://cran.r-project.org/web/packages/forecast/index.html

Ilstedt U, Bargués Tobella A, Bazié HR, Bayala J, Verbeeten E, Nyberg G, Sanou J, Benegas L, Murdiyarso D, Laudon H, Sheil D, Malmer A. 2016. Intermediate tree cover can maximize groundwater recharge in the seasonally dry tropics. Sci Rep 6:21930.

Jackson RB, Banner JL, Jobbágy EG, Pockman WT, Wall DH. 2002. Ecosystem carbon loss with woody plant invasion of grasslands. Nature 418:623–626.

Jarecke KM, Zhang X, Keen RM, Dumont M, Li B, Sadayappan K, Moreno V, Ajami H, Billings SA, Flores AN, Hirmas DR, Kirk MF, Li L, Nippert JB, Singha K, Sullivan PL. 2024. Woody encroachment modifies subsurface structure and hydrological function. Ecohydrology 18:e2731.

Jayawickreme DH, Van Dam RL, Hyndman DW. 2008. Subsurface imaging of vegetation, climate, and root-zone moisture interactions. Geophys Res Lett 35:L18404.

Johnson MS, Lehmann J. 2006. Double-funneling of trees: stemflow and root-induced preferential flow. Écoscience 13:324–333.

Kaiser K, Kalbitz K. 2012. Cycling downwards – dissolved organic matter in soils. Soil Biol Biochem 52:29–32.

Keen RM, Helliker BR, McCulloh KA, Nippert JB. 2024a. Save or spend? Diverging water-use strategies of grasses and encroaching clonal shrubs. J Ecol 112:870–885.

Keen RM, Sadayappan K, Jarecke KM, Li L, Kirk MF, Sullivan PL, Nippert JB. 2024b. Unexpected hydrologic response to ecosystem state change in tallgrass prairie. J Hydrol 643:131937.

Keen RM, Nippert JB, Sullivan PL, Ratajczak Z, Ritchey B, O'Keefe K, Dodds WK. 2023. Impacts of riparian and non-riparian woody encroachment on tallgrass prairie ecohydrology. Ecosystems. https://doi.org/10.1007/s10021-022-00756-7.

Kendall MG. 1948. Rank correlation methods.

Kulmatiski A, Beard KH. 2013a. Root niche partitioning among grasses, saplings, and trees measured using a tracer technique. Oecologia 171:25–37.

Kulmatiski A, Beard KH. 2013b. Woody plant encroachment facilitated by increased precipitation intensity. Nature Clim Change 3:833–837.

LaBrecque DJ, Yang X. 2001. Difference inversion of ERT data: a fast inversion method for 3-D in situ monitoring. J Environ Eng Geophys 6:83–89.

Li H, Shen H, Zhou L, Zhu Y, Chen L, Hu H, Zhang P, Fang J. 2019. Shrub encroachment increases soil carbon and nitrogen stocks in temperate grasslands in China. Land Degrad Dev 30:756–767.

Logan KE, Brunsell NA. 2015. Influence of drought on growing season carbon and water cycling with changing land cover. Agri Forest Meteorol 213:217–225.

Macpherson GL, Sullivan PL. 2019. Watershed-scale chemical weathering in a merokarst terrain, northeastern Kansas, USA. Chem Geol 527:118988.

Maggi F, Porporato A. 2007. Coupled moisture and microbial dynamics in unsaturated soils. Water Resour Res 43:2006WR005367.

Mann HB. 1945. Nonparametric tests against trend. Econometrica 13:245–259.

Niemeyer RJ, Heinse R, Link TE, Seyfried MS, Klos PZ, Williams CJ, Nielson T. 2017. Spatiotemporal soil and saprolite moisture dynamics across a semi-arid woody plant gradient. J Hydrol 544:21–35.

Nippert JB, Knapp AK. 2007. Linking water uptake with rooting patterns in grassland species. Oecologia 153:261–272.

Nippert JB, Wieme RA, Ocheltree TW, Craine JM. 2012. Root characteristics of C4 grasses limit reliance on deep soil water in tallgrass prairie. Plant Soil 355:385–394.

Nippert JB. 2024. ASM01 Soil water content measured by neutron probe at Konza Prairie ver 20.

O'Keefe K, Bachle S, Keen R, Tooley EG, Nippert JB. 2022. Root traits reveal safety and efficiency differences in grasses and shrubs exposed to different fire regimes. Funct Ecol 36:368–379.

Okeefe K, Bell DM, McCulloh KA, Nippert JB. 2020. Bridging the flux gap: Sap flow measurements reveal species-specific patterns of water use in a tallgrass prairie. J Geophys Res Biogeosci 125:e2019JG005446. https://doi.org/10.1029/2019JG005446.

Oldenburg DW, Li Y. 1999. Estimating depth of investigation in DC resistivity and IP surveys. Geophysics 64:403–416.

Patakamuri S, O'Brien N. 2021. Modifiedmk: Modified versions of Mann Kendall and Spearman's Rho trend tests. https://cran.r-project.org/web/packages/modifiedmk/index.html

Ratajczak Z, Nippert JB, Briggs JM, Blair JM. 2014. Fire dynamics distinguish grasslands, shrublands and woodlands as alternative attractors in the Central Great Plains of North America. J Ecol 102:1374–1385.

Ratajczak Z, Collins SL, Blair JM, Koerner SE, Louthan AM, Smith MD, Taylor JH, Nippert JB. 2022. Reintroducing bison results in long-running and resilient increases in grassland diversity. Proc Natl Acad Sci USA 119:e2210433119.

Ratajczak Z, Nippert JB, Hartman JC, Ocheltree TW. 2011. Positive feedbacks amplify rates of woody encroachment in mesic tallgrass prairie. Ecosphere 2:art121.

Sadayappan K, Keen R, Jarecke KM, Moreno V, Nippert JB, Kirk MF, Sullivan PL, Li L. 2023. Drier streams despite a wetter climate in woody-encroached grasslands. J Hydrol 627:130388.

Sang J, Lakshani MMT, Chamindu Deepagoda TKK, Shen Y, Li Y. 2022. Drying and rewetting cycles increased soil carbon dioxide rather than nitrous oxide emissions: a meta-analysis. J Environ Manag 324:116391.

Schmidt HE, Osorio Leyton JM, Popescu SC, Noa Yarasca E, Sarkar S, Wilcox BP. 2024. Connecting the dots: how eco-hydrological connectivity can support remote sensing and modeling to inform management of woody plant encroachment. Rangeland Ecol Manag 95:84–99.

Schreiner-McGraw AP, Vivoni ER, Ajami H, Sala OE, Throop HL, Peters DPC. 2020. Woody plant encroachment has a larger impact than climate change on dryland water budgets. Sci Rep 10:8112.

Scott RL, Huxman TE, Williams DG, Goodrich DC. 2006. Eco-hydrological impacts of woody-plant encroachment: seasonal patterns of water and carbon dioxide exchange within a semiarid riparian environment. Global Change Biol 12:311–324.

Souza LFT, Hirmas DR, Sullivan PL, Reuman DC, Kirk MF, Li L, Ajami H, Wen H, Sarto MVM, Loecke TD, Rudick AK, Rice CW, Billings SA. 2023. Root distributions, precipitation, and soil structure converge to govern soil organic carbon depth distributions. Geoderma 437:116569.

Stevens N, Lehmann CER, Murphy BP, Durigan G. 2017. Savanna woody encroachment is widespread across three continents. Global Change Biol 23:235–244.

Sullivan PL, Stops MW, Macpherson GL, Li L, Hirmas DR, Dodds WK. 2019. How landscape heterogeneity governs stream water concentration-discharge behavior in carbonate terrains (Konza Prairie, USA). Chem Geol 527:118989.

Sullivan PL, Zhang C, Behm M, Zhang F, Macpherson GL. 2020. Toward a new conceptual model for groundwater flow in

merokarst systems: insights from multiple geophysical approaches. Hydrol Process 34:4697–4711.

Sullivan P, Jarecke K. 2024. WES01 Woody encroachment impacts on the subsurface at Konza Prairie.

Swain DL, Prein AF, Abatzoglou JT, Albano CM, Brunner M, Diffenbaugh NS, Singh D, Skinner CB, Touma D. 2025. Hydroclimate volatility on a warming Earth. Nat Rev Earth Environ 6:35–50.

Tiedje JM, Sexstone AJ, Parkin TB, Revsbech NP. 1984. Anaerobic processes in soil. Plant and Soil 76:197–212.

Tiemann LK, Billings SA. 2011. Changes in variability of soil moisture alter microbial community C and N resource use. Soil Biol Biochem 43:1837–1847.

Tooley EG, Nippert JB, Bachle S, Keen RM. 2022. Intra-canopy leaf trait variation facilitates high leaf area index and compensatory growth in a clonal woody encroaching shrub. Tree Physiol 42:tpac078.

Veen GF, Blair JM, Smith MD, Collins SL. 2008. Influence of grazing and fire frequency on small-scale plant community structure and resource. Oikos 117:859–66.

Vero SE, Macpherson GL, Sullivan PL, Brookfield AE, Nippert JB, Kirk MF, Datta S, Kempton P. 2017. Developing a conceptual framework of landscape and hydrology on tallgrass prairie: a critical zone approach. Vadose Zone J 17:1–11.

Wedel ER, Ratajczak Z, Tooley EG, Nippert JB. 2024. Divergent resource-use strategies of encroaching shrubs: Can traits predict encroachment success in tallgrass prairie? J Ecol 113:1365–2745.

Wen H, Perdrial J, Abbott BW, Bernal S, Dupas R, Godsey SE, Harpold A, Rizzo D, Underwood K, Adler T, Sterle G, Li L. 2020. Temperature controls production but hydrology regulates export of dissolved organic carbon at the catchment scale. Hydrol Earth Syst Sci 24:945–966.

Wen H, Sullivan PL, Billings SA, Ajami H, Cueva A, Flores A, Hirmas DR, Koop AN, Murenbeeld K, Zhang X, Li L. 2022. From soils to streams: Connecting terrestrial carbon transformation, chemical weathering, and solute export across hydrological regimes. Water Resour Res 58:e2022WR032314.

Wilcox BP, Basant S, Olariu H, Leite PAM. 2022. Ecohydrological connectivity: A unifying framework for understanding how woody plant encroachment alters the water cycle in drylands. Front Environ Sci 10:934535.

Zou CB, Turton DJ, Will RE, Engle DM, Fuhlendorf SD. 2014. Alteration of hydrological processes and streamflow with juniper (*Juniperus virginiana*) encroachment in a mesic grassland catchment. Hydrol Process 28:6173–6182.

Zou CB, Twidwell D, Bielski CH, Fogarty DT, Mittelstet AR, Starks PJ, Will RE, Zhong Y, Acharya BS. 2018. Impact of eastern redcedar proliferation on water resources in the great plains USA—Current state of knowledge. Water 10:1768.